

# Signature of Lepton flavor universality violation in $B_s \rightarrow D_s \tau \nu$ semileptonic decays

Rupak Dutta\* and Rajeev. N†

National Institute of Technology Silchar, Silchar 788010, India

Deviation from the standard model prediction is observed in many semileptonic  $B$  decays mediated via  $b \rightarrow c$  charged current interactions. In particular, current experimental measurements of the ratio of branching ratio  $R_D$  and  $R_{D^*}$  in  $B \rightarrow D^{(*)} l \nu$  decays disagree with standard model expectations at the level of about  $4.1\sigma$ . Moreover, recent measurement of the ratio of branching ratio  $R_{J/\Psi}$  by LHCb, where  $R_{J/\Psi} = \mathcal{B}(B_c \rightarrow J/\Psi \tau \nu) / \mathcal{B}(B_c \rightarrow J/\Psi \mu \nu)$ , is more than  $2\sigma$  away from the standard model prediction. In this context, we consider an effective Lagrangian in the presence of vector and scalar new physics couplings to study the implications of  $R_D$  and  $R_{D^*}$  anomalies in  $B_s \rightarrow D_s \tau \nu$  decays. We give prediction of several observables such as branching ratio, ratio of branching ratio, forward backward asymmetry parameter,  $\tau$  polarization fraction, and the convexity parameter for the  $B_s \rightarrow D_s \tau \nu$  decays within the standard model and within various new physics scenarios.

PACS numbers: 14.40.Nd, 13.20.He, 13.20.-v

## I. INTRODUCTION

There are several reasons to believe that standard model (SM) of particle physics is not a complete theory, and thus there must be physics beyond the SM. It is therefore crucial to find the pattern of the New Physics (NP) that is responsible for various long standing anomalies. The underlying framework of SM assumes that the charge and neutral leptons are universal in the weak interaction. However, various recent studies on semileptonic  $B$  decays such as  $B \rightarrow D^{(*)} l \nu$ , with  $l$  either  $e$ ,  $\mu$ , or  $\tau$ , challenged the lepton flavor universality [1]. From past few years, many experiments such as  $B$ -factories have reported observables that are deviating from the SM prediction. In particular, the ratio of branching ratio  $R_D$  and  $R_{D^*}$  in  $B \rightarrow D^{(*)} l \nu$  are measured to have large discrepancy with respect to its SM counterpart.

A very precise SM prediction of the ratio of branching ratio  $R_D$  in  $B \rightarrow D l \nu$  using the form factors obtained in lattice quantum chromodynamics (QCD) is reported to be  $0.300 \pm 0.008$  [2–5]. Similarly for  $R_{D^*}$ , it was reported to be  $0.252 \pm 0.003$  [6]. Comparing with the current world average of  $R_D = 0.403 \pm 0.040 \pm 0.024$  and  $R_{D^*} = 0.310 \pm 0.015 \pm 0.008$  from BABAR [7], Belle [8–10], and LHCb [11], the combined deviation currently stands at about  $4.1\sigma$ . For definiteness, we report in Table-I the current status of experimentally measured ratio of branching ratio  $R_D$  and  $R_{D^*}$  [12]. Various studies in explaining the observed anomalies in  $B$  meson decays can be found in [13–41]. Very recently, LHCb has measured the ratio of branching ratio  $R_{J/\psi}$  to be  $0.71 \pm 0.17 \pm 0.18$  [42]. Comparing with the SM prediction [43–45], we find the deviation to be at more than  $2\sigma$ . Although a precise calculation of  $B_c \rightarrow J/\Psi$  form factors is not available at present, a preliminary results for the form factors are provided by HPQCD collaboration using Lattice QCD [46].

Inspired by the anomalies present in  $B \rightarrow (D, D^*) \tau \nu$  decays, we study the corresponding  $B_s \rightarrow D_s \tau \nu$  semileptonic

Experiments	$R_{D^*}$	$R_D$
BABAR	$0.332 \pm 0.024 \pm 0.018$	$0.440 \pm 0.058 \pm 0.042$
BELLE	$0.293 \pm 0.038 \pm 0.015$	$0.375 \pm 0.064 \pm 0.026$
BELLE	$0.302 \pm 0.030 \pm 0.011$	
LHCb	$0.336 \pm 0.027 \pm 0.030$	
BELLE	$0.270 \pm 0.035^{+0.028}_{-0.025}$	
LHCb	$0.285 \pm 0.019 \pm 0.029$	
AVERAGE	$0.304 \pm 0.013 \pm 0.007$	$0.407 \pm 0.039 \pm 0.024$

TABLE I: Current status of  $R_D$  and  $R_{D^*}$  [12].

\*Electronic address: rupak@phy.nits.ac.in

†Electronic address: 16-3-24-102@student.nits.ac.in

decays within SM and within various NP scenarios. A systematic study of  $B_s \rightarrow D_s \tau \nu$  decays is important for several reasons: first, in the limit of SU(3) flavor symmetry,  $B_s \rightarrow D_s \tau \nu$  and  $B \rightarrow D \tau \nu$  decay modes should show similar properties. Second, since  $B \rightarrow (D, D^*) \tau \nu$  and  $B_s \rightarrow D_s \tau \nu$  decays are mediated via  $b \rightarrow c$  charged current interaction, hence anomalies present in  $B \rightarrow (D, D^*) \tau \nu$  should show up in  $B_s \rightarrow D_s \tau \nu$  mode as well. Again, a combined analysis of  $B$  and  $B_s$  meson decays theoretically and experimentally may help us to determine  $|V_{cb}|$  with higher precision and this may also give some hints on our understanding of inclusive and exclusive determination of  $|V_{cb}|$ . The semileptonic  $B_s \rightarrow D_s l \nu$  decays has been studied by various authors [47–58]. Within the SM, the branching ratio and ratio of branching ratio have been calculated using the form factors obtained from perturbative QCD (pQCD), Constituent Quark Meson (CQM) model, covariant light-front quark model, light cone sum rule, and more recently from Lattice QCD. Our main motivation here is to study the implications of  $R_D$  and  $R_{D^*}$  anomalies on  $B_s \rightarrow D_s \tau \nu$  decays in a model independent way. To this end, we use an effective theory formalism in the presence of NP to give prediction on various observables such as the decay rate, ratio of branching ratio, lepton side forward backward asymmetry, longitudinal polarization fraction of the lepton, and the convexity parameter for the  $B_s \rightarrow D_s \tau \nu$  decays. We follow Ref. [59] for various  $B_s \rightarrow D_s$  transition form factors. For our NP analysis, we impose  $1\sigma$  constraint coming from the measured ratio of branching ratio  $R_D$  and  $R_{D^*}$  to obtain the allowed NP parameter space. This is to ensure that the resulting NP parameter space can simultaneously explain the anomalies present in  $R_D$  and  $R_{D^*}$ . We also use the constraint coming from the  $B_c$  meson life time in our analysis as it is shown in Ref. [37] that life time of  $B_c$  meson put severe constraint on various NP couplings. Based on various SM calculation [60–62] of the  $B_c$  life time, it is found that  $\mathcal{B}(B_c \rightarrow \tau \nu)$  can not be more than 5%. However, this can be relaxed up to 30% depending on the input parameters that are used in the SM calculation. Very recently, in Ref. [63] a more stringent bound of  $\mathcal{B}(B_c \rightarrow \tau \nu) \leq 10\%$  was obtained using the LEP data at the  $Z$  peak.

The present discussion is organized as follows. In section. II, we start with a brief discussion of the most general effective Lagrangian in the presence of NP for the  $b \rightarrow c l \nu$  quark level transition decays. The three body differential decay width formula obtained using helicity formalism is also reported in the section. II. Explicit formulas of various observables such as ratio of branching ratio, lepton side forward backward asymmetry,  $\tau$  polarization fraction, and the convexity parameter for the  $B_s \rightarrow D_s \tau \nu$  decays in the presence of NP are reported. In section. III, we first report all the input parameters that are relevant for our numerical computation. Standard model results and the effects of NP couplings on various observables under various NP scenarios are reported in section. III. Finally, we conclude and summarize our results in section. IV.

## II. PHENOMENOLOGY

The natural way to introduce NP effects in a model independent approach is to construct a effective Lagrangian for the weak decays that includes both SM and the beyond the SM physics. We follow Refs. [64, 65] and write the effective weak Lagrangian for the  $b \rightarrow c \tau \nu$  quark level transition decays in the presence of vector and scalar type NP interactions as

$$\begin{aligned} \mathcal{L}_{\text{eff}} = & -\frac{4G_F}{\sqrt{2}} V_{cb} \left\{ (1 + V_L) \bar{l}_L \gamma_\mu \nu_L \bar{c}_L \gamma^\mu b_L + V_R \bar{l}_L \gamma_\mu \nu_L \bar{c}_R \gamma^\mu b_R + \tilde{V}_L \bar{l}_R \gamma_\mu \nu_R \bar{c}_L \gamma^\mu b_L \right. \\ & \left. + \tilde{V}_R \bar{l}_R \gamma_\mu \nu_R \bar{c}_R \gamma^\mu b_R + S_L \bar{l}_R \nu_L \bar{c}_R b_L + S_R \bar{l}_R \nu_L \bar{c}_L b_R + \tilde{S}_L \bar{l}_L \nu_R \bar{c}_R b_L + \tilde{S}_R \bar{l}_L \nu_R \bar{c}_L b_R \right\} + \text{h.c.}, \quad (1) \end{aligned}$$

where,  $G_F$  is the Fermi coupling constant and  $|V_{cb}|$  is the Cabibbo-Kobayashi-Mashkawa (CKM) matrix element. The effective Lagrangian of Eq. 1 is considered at renormalization scale  $\mu = m_b$ . The NP Wilson coefficients (WCs) denoted by  $V_L$ ,  $V_R$ ,  $S_L$ , and  $S_R$  involve left-handed neutrinos, whereas, the WCs denoted by  $\tilde{V}_L$ ,  $\tilde{V}_R$ ,  $\tilde{S}_L$ , and  $\tilde{S}_R$  involve right-handed neutrinos, respectively. Assuming all NP WCs to be real in the present analysis we rewrite the above equation as [13],

$$\begin{aligned} \mathcal{L}_{\text{eff}} = & -\frac{G_F}{\sqrt{2}} V_{cb} \left\{ G_V \bar{l} \gamma_\mu (1 - \gamma_5) \nu_l \bar{c} \gamma^\mu b - G_A \bar{l} \gamma_\mu (1 - \gamma_5) \nu_l \bar{c} \gamma^\mu \gamma_5 b + G_S \bar{l} (1 - \gamma_5) \nu_l \bar{c} b \right. \\ & - G_P \bar{l} (1 - \gamma_5) \nu_l \bar{c} \gamma_5 b + \tilde{G}_V \bar{l} \gamma_\mu (1 + \gamma_5) \nu_l \bar{c} \gamma^\mu b - \tilde{G}_A \bar{l} \gamma_\mu (1 + \gamma_5) \nu_l \bar{c} \gamma^\mu \gamma_5 b \\ & \left. + \tilde{G}_S \bar{l} (1 + \gamma_5) \nu_l \bar{c} b - \tilde{G}_P \bar{l} (1 + \gamma_5) \nu_l \bar{c} \gamma_5 b \right\} + \text{h.c.}, \quad (2) \end{aligned}$$

where,

$$\begin{aligned} G_V &= 1 + V_L + V_R, & G_A &= 1 + V_L - V_R, & G_S &= S_L + S_R, & G_P &= S_L - S_R, \\ \tilde{G}_V &= \tilde{V}_L + \tilde{V}_R, & \tilde{G}_A &= \tilde{V}_L - \tilde{V}_R, & \tilde{G}_S &= \tilde{S}_L + \tilde{S}_R, & \tilde{G}_P &= \tilde{S}_L - \tilde{S}_R. \end{aligned} \quad (3)$$

The  $B_s \rightarrow D_s l \nu$  decay amplitude depends on non perturbative hadronic matrix element which can be parametrized in terms of  $B_s \rightarrow D_s$  transition form factors as follows.

$$\begin{aligned} \langle D_s(P_{D_s}) | \bar{c} \gamma^\mu b | B_s(P_{B_s}) \rangle &= f_+(q^2) \left[ P_{B_s}^\mu + P_{D_s}^\mu - \frac{M_{B_s}^2 - M_{D_s}^2}{q^2} q^\mu \right] + f_0(q^2) \frac{M_{B_s}^2 - M_{D_s}^2}{q^2} q^\mu, \\ \langle D_s(P_{D_s}) | \bar{c} b | B_s(P_{B_s}) \rangle &= \frac{m_{B_s}^2 - m_{D_s}^2}{m_b(\mu) - m_c(\mu)} f_0(q^2), \end{aligned} \quad (4)$$

where,  $q^\mu = P_{B_s}^\mu - P_{D_s}^\mu$  refers to the momentum transfer. It should be mentioned that we use the equation of motion to find the scalar matrix element. We follow Ref. [59] for the relevant form factors  $f_0(q^2)$  and  $f_+(q^2)$ . The expressions pertinent for our discussion are [59]

$$P_0(q^2) f_0(q^2) = \sum_{j=0}^3 a_j^{(0)} z^j, \quad P_+(q^2) f_+(q^2) = \sum_{j=0}^3 a_j^{(+)} \left[ z^j - (-1)^{j-J} \frac{j}{J} z^J \right] \quad (5)$$

where

$$z(q^2) = \frac{\sqrt{t_+ - q^2} - \sqrt{t_+ - t_0}}{\sqrt{t_+ - q^2} + \sqrt{t_+ - t_0}} \quad t_+ = (M_{B_s} + M_{D_s})^2 \quad t_0 = (M_{B_s} - M_{D_s})^2 \quad P_{0,+}(q^2) = 1 - \frac{q^2}{M_{0,+}^2}. \quad (6)$$

Here,  $P_{0,+}$  are Blaschke factors and  $M_0 = 6.42(10)$  GeV and  $M_+ = 6.330(9)$  GeV are the resonance masses. We refer to Ref. [59] for all the omitted details.

The differential decay distribution for the  $B_s \rightarrow D_s l \nu$  decays can be expressed as

$$\frac{d\Gamma}{dq^2 d\cos\theta} = \frac{G_F^2 |V_{cb}|^2 |\vec{P}_{D_s}|}{(2\pi)^3 64 m_{B_s}^2} \left( 1 - \frac{m_l^2}{q^2} \right) L_{\mu\nu} H^{\mu\nu}, \quad (7)$$

where  $|\vec{P}_{D_s}| = \sqrt{\lambda(m_{B_s}^2, m_{D_s}^2, q^2)}/2m_{B_s}$  is the three momentum vector of the outgoing meson and  $\lambda(a, b, c) = a^2 + b^2 + c^2 - 2(ab + bc + ca)$ . Note that  $\theta$  denotes the angle between the  $D_s$  meson and the lepton three momentum vector in the  $(l \nu)$  rest frame. The covariant contraction  $L_{\mu\nu} H^{\mu\nu}$  can be calculated using the helicity techniques of Refs. [66, 67]. For completeness, we present here the final expression for the differential decay distribution of three body  $B_s \rightarrow D_s l \nu$  decays [13].

$$\frac{d\Gamma}{dq^2 d\cos\theta} = 2 N |\vec{P}_{D_s}| \left\{ H_0^2 \sin^2 \theta (G_V^2 + \tilde{G}_V^2) + \frac{m_l^2}{q^2} \left[ (H_0 G_V \cos \theta - H_{tS})^2 + (H_0 \tilde{G}_V \cos \theta - \tilde{H}_{tS})^2 \right] \right\}, \quad (8)$$

where

$$\begin{aligned} N &= \frac{G_F^2 |V_{cb}|^2 q^2}{256 \pi^3 m_{B_s}^2} \left( 1 - \frac{m_l^2}{q^2} \right)^2, & H_0 &= \frac{2 m_{B_s} |\vec{P}_{D_s}|}{\sqrt{q^2}} f_+(q^2), & H_t &= \frac{m_{B_s}^2 - m_{D_s}^2}{\sqrt{q^2}} f_0(q^2), \\ H_S &= \frac{m_{B_s}^2 - m_{D_s}^2}{m_b(\mu) - m_c(\mu)} f_0(q^2), & H_{tS} &= H_t G_V + \frac{\sqrt{q^2}}{m_l} H_S G_S, & \tilde{H}_{tS} &= H_t \tilde{G}_V + \frac{\sqrt{q^2}}{m_l} H_S \tilde{G}_S. \end{aligned} \quad (9)$$

By performing the  $\cos \theta$  integration in Eq. 8, we get

$$\frac{d\Gamma}{dq^2} = \frac{8 N |\vec{P}_{D_s}|}{3} \left\{ H_0^2 \left( G_V^2 + \tilde{G}_V^2 \right) \left( 1 + \frac{m_l^2}{2 q^2} \right) + \frac{3 m_l^2}{2 q^2} \left( H_{tS}^2 + \tilde{H}_{tS}^2 \right) \right\}. \quad (10)$$

Setting  $G_V = G_A = 1$  and all other NP couplings to zero, we obtain

$$\left( \frac{d\Gamma}{dq^2} \right)_{\text{SM}} = \frac{8 N |\vec{P}_{D_s}|}{3} \left\{ H_0^2 \left( 1 + \frac{m_l^2}{2 q^2} \right) + \frac{3 m_l^2}{2 q^2} H_t^2 \right\}. \quad (11)$$

We define several  $q^2$  dependent observables such as differential branching ratio  $\text{DBR}(q^2)$ , ratio of branching ratio  $R(q^2)$ , lepton side forward backward asymmetry  $A_{FB}^l(q^2)$ , polarization fraction of the charged lepton  $P_l(q^2)$ , and convexity parameter  $C_F^l(q^2)$  for the  $B_s \rightarrow D_s l \nu$  decays. Those are

$$\begin{aligned} \text{DBR}(q^2) &= \frac{d\Gamma/dq^2}{\Gamma_{\text{Tot}}}, & R(q^2) &= \frac{\mathcal{B}(B_s \rightarrow D_s \tau \nu)}{\mathcal{B}(B_s \rightarrow D_s l \nu)}, & A_{FB}(q^2) &= \frac{\left(\int_{-1}^0 - \int_0^1\right) d \cos \theta \frac{d\Gamma}{dq^2 d \cos \theta}}{\frac{d\Gamma}{dq^2}}, \\ P_l(q^2) &= \frac{d\Gamma(+)/dq^2 - d\Gamma(-)/dq^2}{d\Gamma(+)/dq^2 + d\Gamma(-)/dq^2}, & C_F^l(q^2) &= \frac{1}{(d\Gamma/dq^2)} \left( \frac{d}{d \cos \theta} \right)^2 \left[ \frac{d\Gamma}{dq^2 d \cos \theta} \right], \end{aligned} \quad (12)$$

where  $d\Gamma(+)/dq^2$  and  $d\Gamma(-)/dq^2$  represent differential decay width of positive and negative helicity leptons, respectively. In the presence of various NP, the explicit expressions for  $A_{FB}^l$ ,  $d\Gamma(+)/dq^2$ ,  $d\Gamma(-)/dq^2$ , and  $C_F^l$  are

$$\begin{aligned} A_{FB}^l(q^2) &= \frac{3m_l^2}{2q^2} \frac{H_0 G_V H_{tS} + H_0 \tilde{G}_V \tilde{H}_{tS}}{H_0^2 (G_V^2 + \tilde{G}_V^2) \left(1 + \frac{m_l^2}{q^2}\right) + \frac{3m_l^2}{2q^2} (H_{tS}^2 + \tilde{H}_{tS}^2)}, \\ \frac{d\Gamma(+)}{dq^2} &= \frac{8N|P_{D_s}^{\vec{}}|}{3} \left[ H_0^2 \tilde{G}_V^2 + \frac{m_l^2}{2q^2} (H_0^2 G_V^2 + 3H_{tS}^2) \right] \\ \frac{d\Gamma(-)}{dq^2} &= \frac{8N|P_{D_s}^{\vec{}}|}{3} \left[ H_0^2 G_V^2 + \frac{m_l^2}{2q^2} (H_0^2 \tilde{G}_V^2 + 3\tilde{H}_{tS}^2) \right], \\ C_F^l &= \frac{3}{2} \frac{H_0^2 (G_V^2 + \tilde{G}_V^2) \left(\frac{m_l^2}{q^2} - 1\right)}{\left[ H_0^2 (G_V^2 + \tilde{G}_V^2) \left(1 + \frac{m_l^2}{2q^2}\right) + \frac{3m_l^2}{2q^2} (H_{tS}^2 + \tilde{H}_{tS}^2) \right]} \end{aligned} \quad (13)$$

The SM expressions are obtained by setting all the NP couplings to zero.

$$\begin{aligned} [A_{FB}^l(q^2)]_{SM} &= \frac{3m_l^2}{2q^2} \left\{ \frac{H_0 H_t}{H_0^2 \left(1 + \frac{m_l^2}{q^2}\right) + \frac{3m_l^2}{2q^2} H_t^2} \right\}, & [P^l]_{SM} &= \frac{\frac{m_l^2}{2q^2} (H_0^2 + 3H_t^2) - H_0^2}{\frac{m_l^2}{2q^2} (H_0^2 + 3H_t^2) + H_0^2}, \\ [C_F^l]_{SM} &= \frac{3}{2} \frac{H_0^2 \left(\frac{m_l^2}{q^2} - 1\right)}{\left[ H_0^2 \left(1 + \frac{m_l^2}{2q^2}\right) + \frac{3m_l^2}{2q^2} H_t^2 \right]} \end{aligned} \quad (14)$$

The average values of the forward-backward asymmetry of the charged lepton  $\langle A_{FB}^l \rangle$ , the longitudinal polarization fraction of the lepton  $\langle P^l \rangle$ , and the convexity parameter  $\langle C_F^l \rangle$  are obtained by separately integrating the numerators and denominators over  $q^2$ .

### III. NUMERICAL RESULTS AND DISCUSSIONS

#### A. Input parameters

Before proceeding for the analysis, we report in Table-II all the input parameters that are relevant for our numerical computation. For the mass and lifetime parameter, we use the latest values reported in Ref. [68]. Similarly for the CKM matrix element  $|V_{cb}|$  and the Fermi coupling constant  $G_F$ , we use Ref. [68]. The lepton masses ( $m_e$ ,  $m_\tau$ ) and meson masses ( $B_s$ ,  $D_s$ ) are in GeV units, whereas Fermi coupling constant  $G_F$  is in  $\text{GeV}^{-2}$  units. The lifetime of  $B_s$  meson ( $\tau_{B_s}$ ) is in seconds. The quark masses  $m_b(m_b)$  and  $m_c(m_b)$  evaluated at renormalization scale  $\mu = m_b$  are in GeV units. For the relevant  $B_s \rightarrow D_s$  form factor parameters, we follow the most recent Lattice QCD calculation of Ref. [59]. The uncertainties associated with  $|V_{cb}|$ , and the form factors parameters are written within parenthesis. We do not report the uncertainties associated with other input parameters as they do not play an important role in our analysis.

We wish to determine the consequences of various NP couplings on various observables for the  $B_s \rightarrow D_s \tau \nu$  decays in a model independent way. It is, therefore, crucial to determine the size of the SM uncertainties in each observable that may come from various input parameters. Uncertainties in the theoretical prediction of the observables mainly come from two sources. First, it may come from not very well known CKM matrix element  $|V_{cb}|$  and second, it may come from the non perturbative hadronic inputs such as decay constant and meson to meson form factors. To gauge the effect of above mentioned uncertainties on various observables, we use a random number generator and vary these input parameters within  $1\sigma$  of their central values.

Inputs from PDG [68]		Form factor inputs [59]	
$m_{B_s}$	5.36689	$a_0^{(0)}$	0.658(31)
$m_{D_s}$	1.96827	$a_1^{(0)}$	-0.10(30)
$m_b(\mu)$	4.18	$a_2^{(0)}$	1.3(2.8)
$m_c(\mu)$	0.91	$a_0^{(+)}$	0.858(32)
$m_e$	$0.05109989461 \times 10^{-2}$	$a_1^{(+)}$	-3.38(41)
$m_\tau$	1.77682	$a_2^{(+)}$	0.6(4.7)
$ V_{cb} $	0.0409(11)		
$G_F$	$1.1663787 \times 10^{-5}$		
$\tau_{B_s}$	$1.505 \times 10^{-12}$		

TABLE II: Theory inputs

### B. Standard model prediction

First, we wish to give prediction of various observables for both the  $e$  and  $\tau$  mode within the SM. We report in Table.-III the SM central values and the  $1\sigma$  ranges of each observable for the  $e$  and the  $\tau$  modes. Here, the central values are obtained by considering only the central values of theory input parameters whereas, the  $1\sigma$  ranges of each observable is obtained by performing a random scan of the hadronic parameters and the CKM matrix element within  $1\sigma$  of their central values. The value of ratio of branching ratio  $R_{D_s}$  in Table.-III is quite similar to the value reported in Ref. [59]. The slight difference may come from different choices of input parameters.

Observables	Central value	$1\sigma$ range	Observables	Central value	$1\sigma$ range	Observables	Central value	$1\sigma$ range
$\mathcal{B}(B_s \rightarrow D_s e \nu)\%$	2.238	[1.839, 2.693]	$P^e$	-1.00	-1.00	$P^\tau$	0.320	[0.234, 0.403]
$\mathcal{B}(B_s \rightarrow D_s \tau \nu)\%$	0.670	[0.573, 0.777]	$A_{FB}^e$	0.00	0.00	$A_{FB}^\tau$	0.360	[0.352, 0.364]
$R_{D_s}$	0.299	[0.260, 0.351]	$C_F^e$	-1.5	-1.50	$C_F^\tau$	-0.271	[-0.239, -0.305]

TABLE III: SM prediction of various observables for the  $e$  and the  $\tau$  modes

We notice that the SM prediction for the  $e$  mode is quite different from the  $\tau$  mode. There is even a sign change in the polarization fraction  $P_l$  while going from the  $e$  to the  $\tau$  mode. Again, the forward backward asymmetry parameter for the  $e$  mode is zero, whereas, it is non zero positive for the  $\tau$  mode. Similarly, the convexity parameter  $C_F^l$  for the  $e$  mode is much larger in magnitude than for the  $\tau$  mode. It is worth mentioning that the mass of the charged lepton plays an important role. In Fig. 1, we show the  $q^2$  dependence of each observable for the  $e$  and the  $\tau$  modes, respectively. We notice that the  $A_{FB}^l(q^2)$ ,  $P^l(q^2)$  and the  $C_F^l(q^2)$  observables remain constant in the entire  $q^2$  region for the  $e$  mode. This could be very well understood from Eq. 14. In the massless limit, i.e, in the  $m_l \rightarrow 0$  limit, the  $q^2$  dependence gets cancelled in the ratio for the  $A_{FB}^l(q^2)$ ,  $P^l(q^2)$  and the  $C_F^l(q^2)$  observables.

Now we proceed to discuss various NP effects in  $B_s \rightarrow D_s \tau \nu$  decays.

### C. New physics in $B_s \rightarrow D_s \tau \nu$ decays

Study of  $B_s \rightarrow D_s \tau \nu$  decays both theoretically and experimentally is well motivated because of the long standing anomalies present in  $R_D$  and  $R_{D^*}$ . We wish to study the implication of these existing anomalies on the  $B_s \rightarrow D_s \tau \nu$  decays in a model independent way. We consider four different NP scenarios based on NP contributions from two different operators. In order to determine the allowed NP parameter space, we impose  $1\sigma$  constraint coming from the measured ratio of branching ratios  $R_D$  and  $R_{D^*}$ . We use the average values of  $R_D$  and  $R_{D^*}$  reported in Table. I in our analysis. For the uncertainties we added the statistical and systematic uncertainties in quadrature. Again, we assume that only the third generation leptons get contribution from NP.

#### 1. Scenario I: only $V_L$ and $V_R$ NP couplings

In this scenario, we vary  $V_L$  and  $V_R$  and set all other NP couplings to zero. This is to ensure that NP contribution to the  $B_s \rightarrow D_s \tau \nu$  decay mode is coming only from vector type NP couplings that involves left handed neutrinos. In

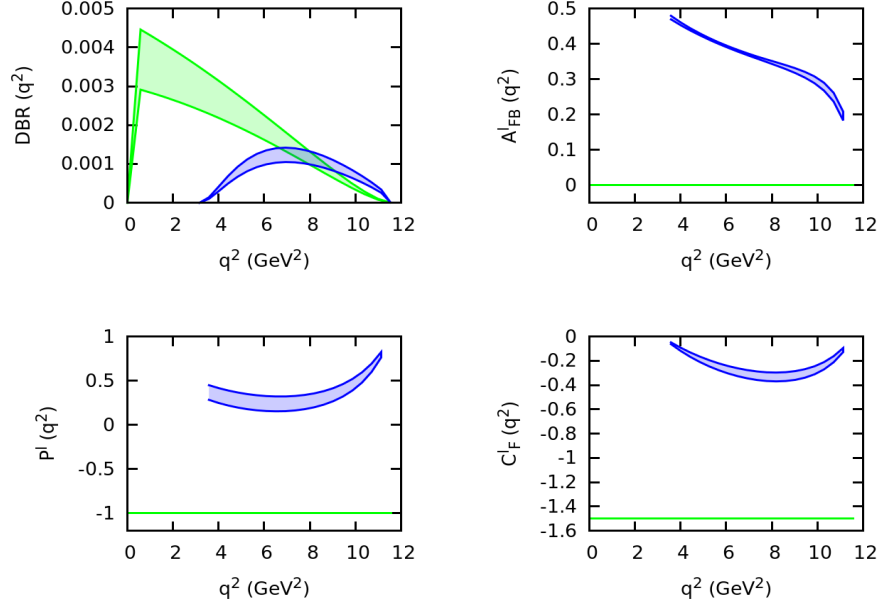


FIG. 1:  $q^2$  dependence of various observables in the SM for the  $e$  (green) and the  $\tau$  (blue) modes.

the presence of such NP, the  $d\Gamma/dq^2$ ,  $R(q^2)$ ,  $A_{FB}^\tau(q^2)$ ,  $P^\tau(q^2)$ , and  $C_F^\tau(q^2)$  can be expressed as

$$\begin{aligned} \left[ \frac{d\Gamma}{dq^2} \right]_{V_{L,R}} &= \left[ \frac{d\Gamma}{dq^2} \right]_{SM} G_V^2, & [R_{D_s}]_{V_{L,R}} &= [R_{D_s}]_{SM} G_V^2, \\ [A_{FB}^l(q^2)]_{V_{L,R}} &= [A_{FB}^l(q^2)]_{SM}, & [P^l]_{V_{L,R}} &= [P^l]_{SM}, & [C_F^l]_{V_{L,R}} &= [C_F^l]_{SM} \end{aligned} \quad (15)$$

It is evident from Eq. 15 that  $d\Gamma/dq^2$  and  $R(q^2)$  depend on  $V_L$  and  $V_R$  NP couplings and are proportional to  $G_V^2$ , whereas,  $P^\tau(q^2)$ ,  $A_{FB}^\tau(q^2)$ , and  $C_F^\tau(q^2)$  do not depend on these NP couplings since the contribution coming from  $V_L$  and  $V_R$  NP couplings gets canceled in the ratio. The allowed ranges of  $V_L$  and  $V_R$  after imposing  $1\sigma$  constraint coming from  $R_D$  and  $R_{D^*}$  are shown in the left panel of Fig. 2. In the right panel we show the corresponding ranges in  $\mathcal{B}(B_c \rightarrow \tau\nu)$  and  $\mathcal{B}(B_s \rightarrow D_s\tau\nu)$ . From the right panel of Fig. 2, we notice that the  $\mathcal{B}(B_c \rightarrow \tau\nu)$  obtained in this scenario lies in the 2% – 3% range. This is consistent with the SM calculation. We report in Table-IV the allowed

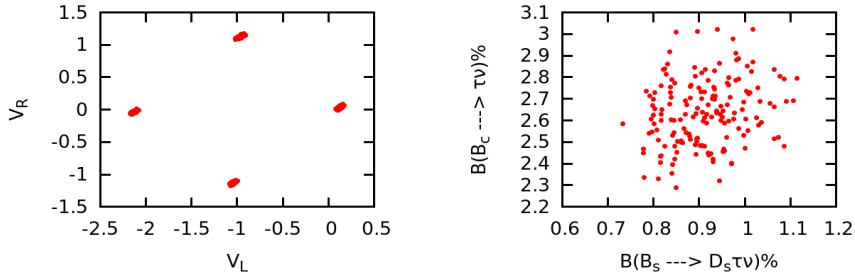
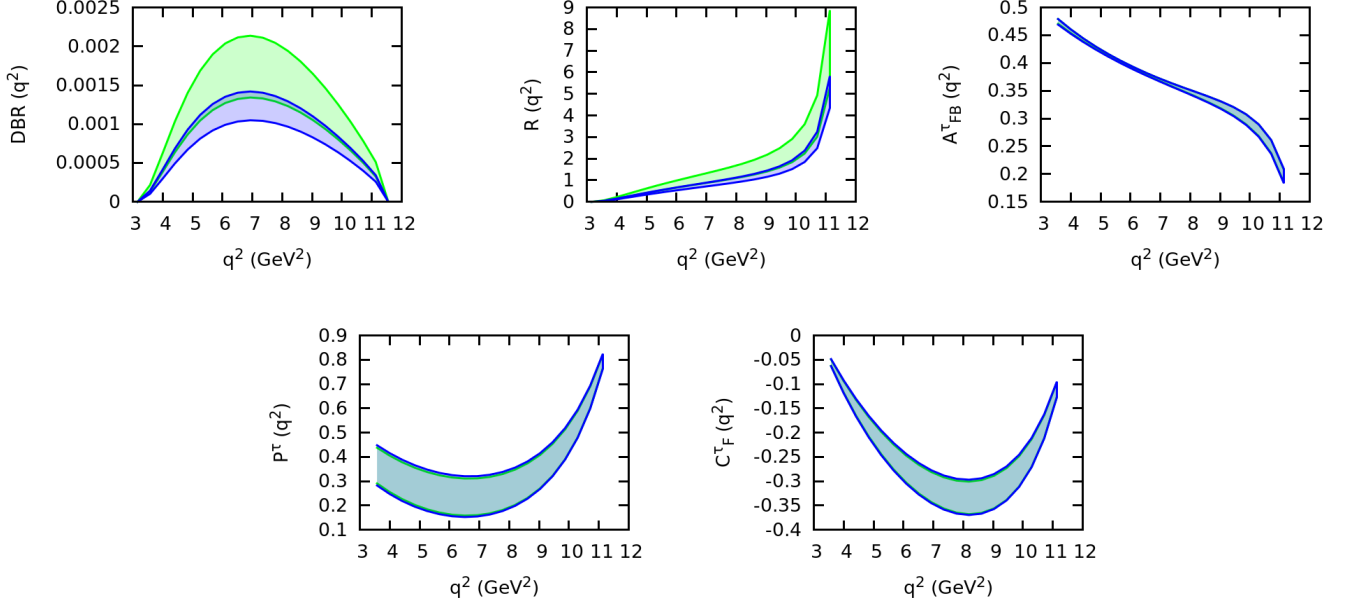


FIG. 2: Allowed ranges of  $V_L$  and  $V_R$  NP couplings are shown in the left panel once  $1\sigma$  constraint coming from the measured values of the ratio of branching ratios  $R_D$  and  $R_{D^*}$  is imposed. We show in the right panel the allowed ranges in  $\mathcal{B}(B_c \rightarrow \tau\nu)$  and  $\mathcal{B}(B_s \rightarrow D_s\tau\nu)$  in the presence of these NP couplings.

ranges of each observable for the  $B_s \rightarrow D_s\tau\nu$  decays with  $(V_L, V_R)$  NP couplings of Fig. 2. We see significant deviation in  $\mathcal{B}(B_s \rightarrow D_s\tau\nu)$  and  $R_{D_s}$  from the SM prediction. As expected, the ranges of  $P_{D_s}^\tau$ ,  $A_{FB}^\tau$ , and  $C_F^\tau$  do not vary at all with such NP couplings.

We show in Fig. 3 the  $q^2$  dependence of various observables with the allowed values of  $V_L$  and  $V_R$  NP couplings of Fig. 2. The SM  $1\sigma$  range is shown with blue band, whereas, the allowed range with  $V_L$  and  $V_R$  NP couplings is

$\mathcal{B}(B_s \rightarrow D_s \tau \nu)\%$	$R_{D_s}$	$P^\tau$	$A_{FB}^\tau$	$C_F^\tau$
[0.733, 1.115]	[0.329, 0.496]	[0.234, 0.403]	[0.352, 0.364]	[-0.239, -0.305]

TABLE IV: Allowed ranges of various observables with  $V_L$  and  $V_R$  NP couplings of Fig. 2.FIG. 3:  $q^2$  dependence of various observables with the allowed ranges of  $V_L$  and  $V_R$  NP couplings of Fig. 2 are shown with green band. The corresponding  $1\sigma$  SM range is shown with the blue band.

shown with green band. It is evident from Fig. 3 that the differential branching ratio  $\text{DBR}(q^2)$  and ratio of branching ratio  $R(q^2)$  deviate considerably from the SM expectation. Again, as expected, we do not observe any deviation of  $A_{FB}^\tau(q^2)$ ,  $P_\tau(q^2)$  and  $C_F^\tau(q^2)$  from the SM expectation in this NP scenario.

## 2. Scenario II: only $S_L$ and $S_R$ NP couplings

In this scenario, we consider the effect of new scalar couplings only, i.e.,  $(S_L, S_R) \neq 0$  and all the other NP couplings are zero. In the presence of  $S_L$  and  $S_R$  NP couplings, the differential decay width, ratio of branching ratio, forward backward asymmetry, polarization fraction of the  $\tau$  lepton, and the convexity parameter can be expressed as

$$\begin{aligned}
\left[\frac{d\Gamma}{dq^2}\right]_{S_{L,R}} &= \left[\frac{d\Gamma}{dq^2}\right]_{SM} + 8N|P_{D_s}| \left( \frac{1}{2}H_S^2 G_S^2 + \frac{m_l}{\sqrt{q^2}} H_t H_S G_S \right), \\
[R_{D_s}]_{S_{L,R}} &= [R_{D_s}]_{SM} + \frac{8N|P_{D_s}| \left( \frac{1}{2}H_S^2 G_S^2 + \frac{m_l}{\sqrt{q^2}} H_t H_S G_S \right)}{\mathcal{B}(B_s \rightarrow D_s e \nu)}, \\
A_{FB}^l(q^2)|_{S_{L,R}} &= \frac{3m_l^2}{2q^2} \left[ \frac{H_0 H_t + H_0 \frac{\sqrt{q^2}}{m_l} H_S G_S}{H_0^2 \left(1 + \frac{m_l^2}{q^2}\right) + \frac{3m_l^2}{2q^2} H_t^2 + (3/2) H_S^2 G_S^2 + 3(m_l/\sqrt{q^2}) H_t H_S G_S} \right], \\
[P^l]_{S_{L,R}} &= \frac{\frac{m_l^2}{2q^2} (H_0^2 + 3H_t^2) - H_0^2 + (3/2) H_S^2 G_S^2 + 3(m_l/\sqrt{q^2}) H_t H_S G_S}{\frac{m_l^2}{2q^2} (H_0^2 + 3H_t^2) + H_0^2 + (3/2) H_S^2 G_S^2 + 3(m_l/\sqrt{q^2}) H_t H_S G_S}, \\
[C_F^l]_{S_{L,R}} &= \frac{3}{2} \frac{H_0^2 \left( \frac{m_l^2}{q^2} - 1 \right)}{\left\{ H_0^2 \left(1 + \frac{m_l^2}{2q^2}\right) + \frac{3m_l^2}{2q^2} H_t^2 \right\} + (3/2) H_S^2 G_S^2 + 3(m_l/\sqrt{q^2}) H_t H_S G_S}
\end{aligned} \tag{16}$$

We impose  $1\sigma$  constraint coming from experimental values of  $R_D$  and  $R_{D^*}$  to determine the allowed values of  $S_L$  and  $S_R$  NP couplings. The resulting  $(S_L, S_R)$  allowed ranges are shown in the left panel of Fig. 4. In the right panel, we show the corresponding ranges in  $\mathcal{B}(B_c \rightarrow \tau\nu)$  and  $\mathcal{B}(B_s \rightarrow D_s\tau\nu)$  obtained using the allowed values of  $(S_L, S_R)$  NP couplings. It should be noted that the  $\mathcal{B}(B_c \rightarrow \tau\nu)$  obtained in this scenario is rather large; more than 30%. Thus, although  $(S_L, S_R)$  NP couplings can simultaneously explain the anomalies present in  $R_D$  and  $R_{D^*}$ , it, however, fails to satisfy the  $\mathcal{B}(B_c \rightarrow \tau\nu) \leq 30\%$  constraint obtained in the SM. Although this particular scenario is ruled out by

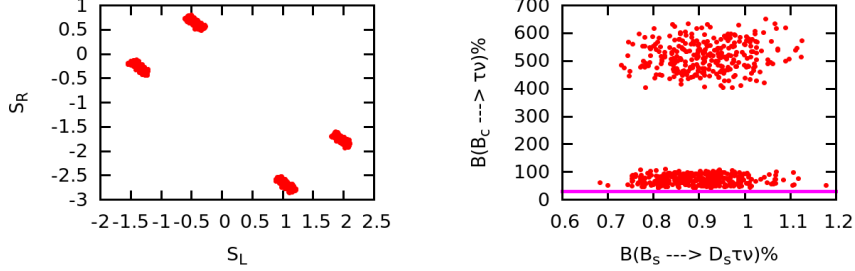


FIG. 4: Allowed ranges of  $S_L$  and  $S_R$  NP couplings are shown in the left panel once  $1\sigma$  constraint coming from the measured values of the ratio of branching ratios  $R_D$  and  $R_{D^*}$  is imposed. We show in the right panel the allowed ranges in  $\mathcal{B}(B_c \rightarrow \tau\nu)$  and  $\mathcal{B}(B_s \rightarrow D_s\tau\nu)$  in the presence of these NP couplings. The pink constant line in the right panel corresponds to the upper bound of  $\mathcal{B}(B_c \rightarrow \tau\nu) = 30\%$  obtained in the SM.

$\mathcal{B}(B_s \rightarrow D_s\tau\nu)\%$	$R_{D_s}$	$P^\tau$	$A_{FB}^\tau$	$C_F^\tau$
[0.683, 1.178]	[0.306, 0.518]	[0.345, 0.609]	[-0.276, 0.355]	[-0.156, -0.260]

TABLE V: Allowed ranges of various observables in the presence of  $S_L$  and  $S_R$  NP couplings

the  $\mathcal{B}(B_c \rightarrow \tau\nu)$  constraint, nevertheless, we report in Table. V the allowed ranges of all the observables obtained using the allowed values of  $S_L$  and  $S_R$  NP couplings of Fig. 4. The deviation from the SM prediction observed in this scenario is quite significant. We notice that the forward backward asymmetry parameter can assume negative values within this scenario, which is quite distinct from SM expectation.

We show the effect of NP on various  $q^2$  dependent observables in Fig. 5. We show with blue the SM  $1\sigma$  band, whereas, we show with green the allowed band once the NP is switched on. The deviation observed in this scenario is rather large and it is, indeed, more pronounced that the deviation obtained with  $(V_L, V_R)$  NP couplings. Unlike scenario I, there is no cancellation of NP effects in  $A_{FB}^\tau(q^2)$ ,  $P^\tau(q^2)$ , and  $C_F^\tau(q^2)$ . We notice that, although there is no zero crossing in the SM for the  $A_{FB}^\tau(q^2)$  parameter, we may observe zero crossing depending on the values of  $S_L$  and  $S_R$  NP couplings. Similar conclusion can be drawn for the  $\tau$  polarization fraction  $P^\tau(q^2)$  as well. Moreover, depending on the values of the NP couplings, shape of the  $q^2$  distribution curve of each observable can be quite different from its SM counterpart.

### 3. Scenario III: only $\tilde{V}_L$ and $\tilde{V}_R$ NP couplings

To study the effect of new vector type NP couplings associated with right handed neutrino interactions, we consider  $(\tilde{V}_L, \tilde{V}_R)$  to be nonzero while all other NP couplings to be zero. In this scenario, the differential decay width, ratio of branching ratio, forward backward asymmetry,  $\tau$  polarization fraction, and the convexity parameter take the following simple form:

$$\begin{aligned}
 \left[ \frac{d\Gamma}{dq^2} \right]_{\tilde{V}_{L,R}} &= \left[ \frac{d\Gamma}{dq^2} \right]_{SM} (1 + \tilde{G}_V^2), & [R_{D_s}]_{\tilde{V}_{L,R}} &= [R_{D_s}]_{SM} (1 + \tilde{G}_V^2), \\
 [A_{FB}^l(q^2)]_{\tilde{V}_{L,R}} &= [A_{FB}^l(q^2)]_{SM}, & [P^l]_{\tilde{V}_{L,R}} &= [P^l]_{SM} \frac{(1 - \tilde{G}_V^2)}{(1 + \tilde{G}_V^2)}, & [C_F^l]_{\tilde{V}_{L,R}} &= [C_F^l]_{SM} \quad (17)
 \end{aligned}$$

In the left panel of Fig. 6 we show the allowed region of  $(\tilde{V}_L, \tilde{V}_R)$  NP couplings that is obtained once  $1\sigma$   $R_D$  and  $R_{D^*}$  experimental constraint is imposed. Similarly, in the right panel we show the corresponding ranges of  $\mathcal{B}(B_c \rightarrow \tau\nu)$  and

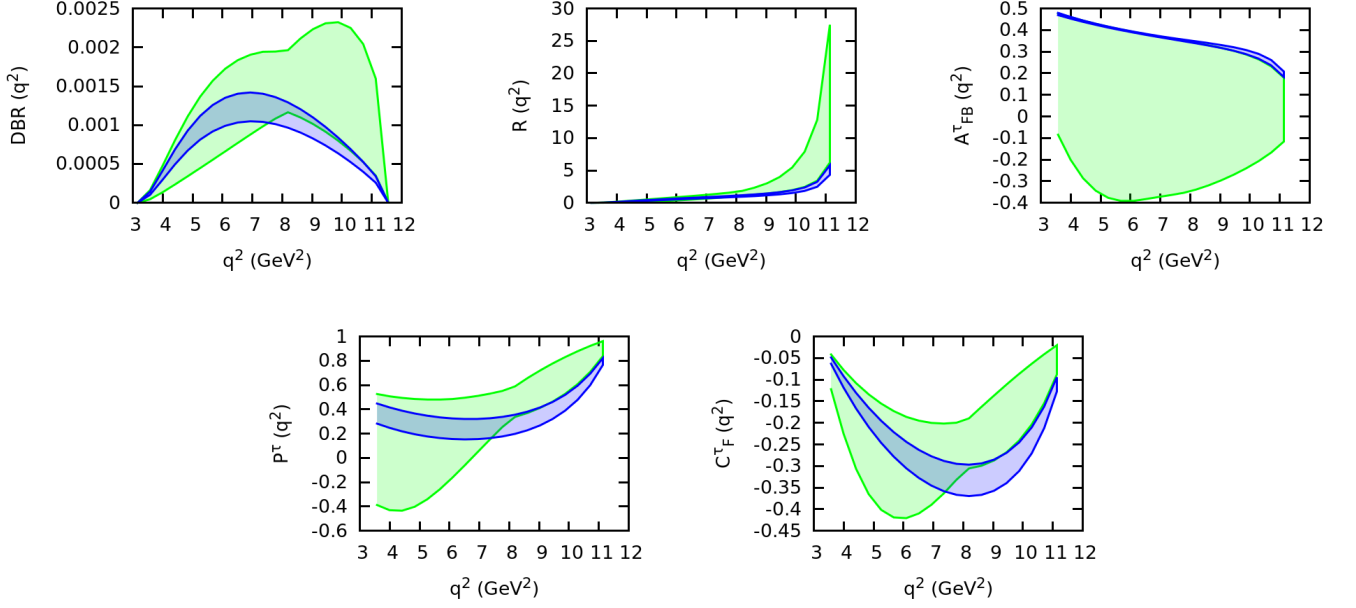


FIG. 5:  $q^2$  dependence of various observables with the allowed ranges of  $S_L$  and  $S_R$  NP couplings of Fig. 4 are shown with green band. The corresponding  $1\sigma$  SM range is shown with the blue band.

$\mathcal{B}(B_s \rightarrow D_s \tau \nu)$  obtained with the  $(\tilde{V}_L, \tilde{V}_R)$  NP couplings. Similar to Scenario I, we notice that  $\mathcal{B}(B_c \rightarrow \tau \nu)$  obtained in this scenario lies within  $(2 - 3)\%$  range. This is, again, consistent with the SM prediction. In Table. VI, we report the possible ranges of all the observables for the  $B_s \rightarrow D_s \tau \nu$  decays. The deviation from the SM prediction observed in this scenario is quite similar to the deviation observed in scenario I. However, there is one subtle difference. Unlike scenario I, a significant deviation from the SM prediction for the  $\tau$  polarization fraction is observed in this scenario. This is evident from Eq. 17 that the NP effect does not get cancelled for the  $\tau$  polarization fraction  $P^\tau$ .

In Fig. 7, we show the variation of various observables such as differential branching ratio, ratio of branching ratio, forward-backward asymmetry,  $\tau$  polarization fraction, and convexity parameter as a function of  $q^2$ . The deviation from the SM prediction observed in this scenario is quite similar to scenario I. As expected, we observe a significant deviation in  $\tau$  polarization parameter in this scenario. All the above mentioned analysis for the observed deviations are clearly reflected in Eq. 17.

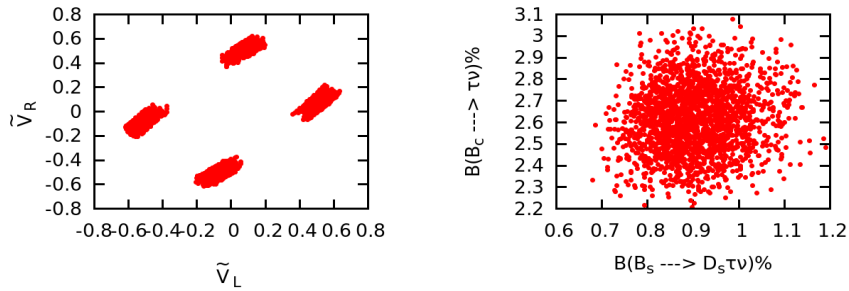
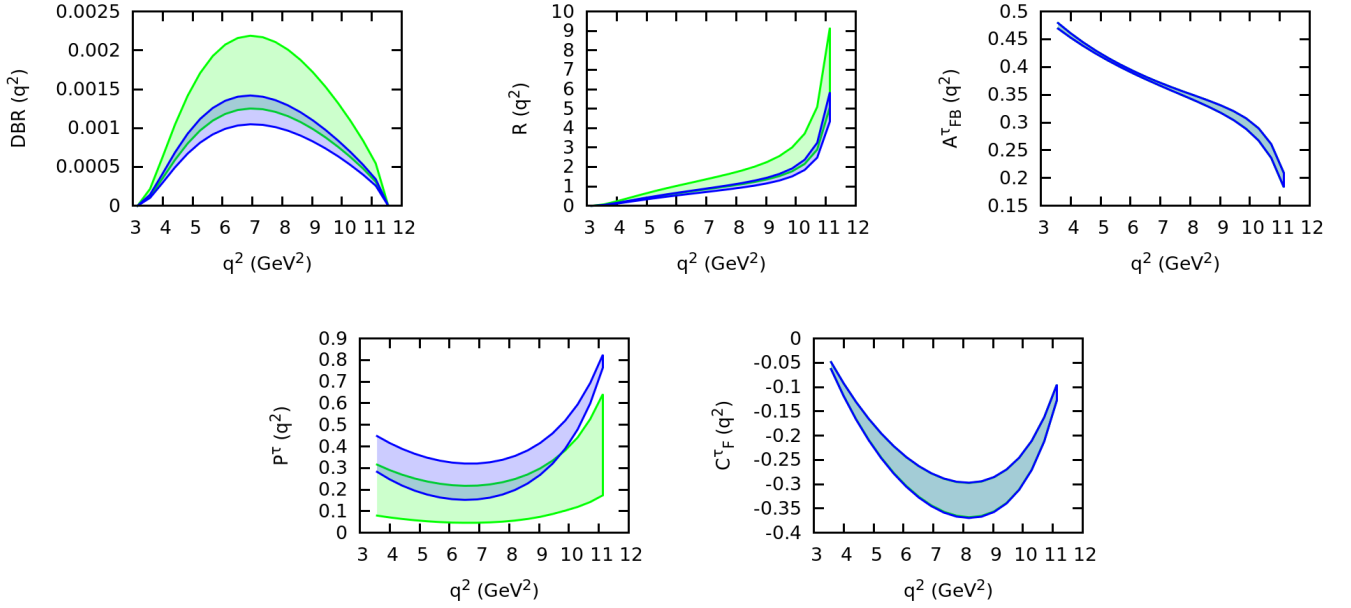


FIG. 6: Allowed ranges of  $\tilde{V}_L$  and  $\tilde{V}_R$  NP couplings are shown in the left panel once  $1\sigma$  constraint coming from the measured values of the ratio of branching ratios  $R_D$  and  $R_{D^*}$  is imposed. We show in the right panel the allowed ranges in  $\mathcal{B}(B_c \rightarrow \tau \nu)$  and  $\mathcal{B}(B_s \rightarrow D_s \tau \nu)$  in the presence of these NP couplings.

$\mathcal{B}(B_s \rightarrow D_s \tau \nu)\%$	$R_{D_s}$	$P^\tau$	$A_{FB}^\tau$	$C_F^\tau$
[0.679, 1.191]	[0.305, 0.525]	[0.064, 0.281]	[0.352, 0.364]	[-0.239, -0.305]

TABLE VI: Allowed ranges of various observables in the presence of  $\tilde{V}_L$  and  $\tilde{V}_R$  NP couplingsFIG. 7:  $q^2$  dependence of various observables with the allowed ranges of  $\tilde{V}_L$  and  $\tilde{V}_R$  NP couplings of Fig. 6 are shown with green band. The corresponding  $1\sigma$  SM range is shown with the blue band.

#### 4. Scenario IV: only $\tilde{S}_L$ and $\tilde{S}_R$ NP couplings

In this scenario, we wish to see the effect of new scalar type NP couplings on various observables. To this end, we consider  $(\tilde{S}_L, \tilde{S}_R)$  to be non zero and all other NP couplings to be zero. In this scenario, the differential decay width, ratio of branching ratio, forward backward asymmetry,  $\tau$  polarization fraction, and the convexity parameter take the following form:

$$\begin{aligned}
\left[\frac{d\Gamma}{dq^2}\right]_{\tilde{S}_{L,R}} &= \left[\frac{d\Gamma}{dq^2}\right]_{SM} + 4N|P_{D_s}|H_S^2\tilde{G}_S^2, & [R_{D_s}]_{\tilde{S}_{L,R}} &= [R_{D_s}]_{SM} + \frac{(3/2)H_S^2\tilde{G}_S^2}{\mathcal{B}(B_s \rightarrow D_s e \nu)}, \\
[A_{FB}^l(q^2)]_{\tilde{S}_{L,R}} &= \frac{3m_l^2}{2q^2} \left[ \frac{H_0 H_t}{H_0^2 \left(1 + \frac{m_l^2}{q^2}\right) + \frac{3m_l^2}{2q^2} H_t^2 + (3/2)H_S^2\tilde{G}_S^2} \right], \\
[P^l]_{\tilde{S}_{L,R}} &= \frac{\frac{m_l^2}{2q^2}(H_0^2 + 3H_t^2) - H_0^2 - (3/2)H_S^2\tilde{G}_S^2}{\frac{m_l^2}{2q^2}(H_0^2 + 3H_t^2) + H_0^2 + (3/2)H_S^2\tilde{G}_S^2}, \\
[C_F^l(q^2)]_{\tilde{S}_{L,R}} &= \frac{3}{2} \frac{H_0^2 \left(\frac{m_l^2}{q^2} - 1\right)}{\left\{H_0^2 \left(1 + \frac{m_l^2}{2q^2}\right) + \frac{3m_l^2}{2q^2} H_t^2\right\} + (3/2)H_S^2\tilde{G}_S^2}
\end{aligned} \tag{18}$$

In order to determine the allowed ranges of  $(\tilde{S}_L, \tilde{S}_R)$  NP couplings, we impose  $1\sigma$  constraint coming from experimentally measured values of  $R_D$  and  $R_{D^*}$ . The resulting NP parameter space, shown in the left panel of Fig. 8, can simultaneously explain the anomalies present in  $R_D$  and  $R_{D^*}$ . We show in the right panel the allowed ranges in  $\mathcal{B}(B_c \rightarrow \tau \nu)$  and  $B_s \rightarrow D_s \tau \nu$  with such NP. We notice that the  $\mathcal{B}(B_c \rightarrow \tau \nu)$  obtained in this scenario is not compatible with the upper bound of  $\mathcal{B}(B_c \rightarrow \tau \nu) \leq 30\%$  obtained in the SM. The numerical values written in the square brackets of Table-VII represent the allowed ranges of observables obtained with the allowed values of  $(\tilde{S}_L, \tilde{S}_R)$

of Fig. 8. Similar to scenario II, we see significant deviation of all the observables from the SM expectation.

We show in Fig. 9 the  $q^2$  distribution of various observables for the  $B_s \rightarrow D_s \tau \nu$  decays. The blue band corresponds to the  $1\sigma$  SM range, whereas, the green band corresponds to the range of the observables once the  $(\tilde{S}_L, \tilde{S}_R)$  NP couplings are switched on. The deviation observed in this scenario is rather large. We notice that although, in the SM, there is no zero crossing in the  $\tau$  polarization parameter, there may or may not be a zero crossing depending on the values of the NP couplings. For the differential branching ratio, the peak of the  $q^2$  distribution may shift towards high  $q^2$  region.

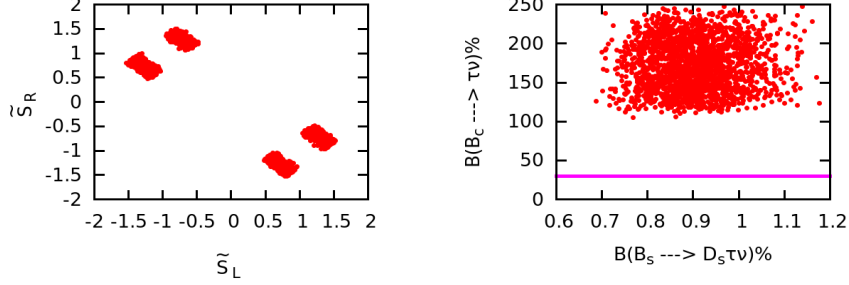


FIG. 8: Allowed ranges of  $\tilde{S}_L$  and  $\tilde{S}_R$  NP couplings are shown in the left panel once  $1\sigma$  constraint coming from the measured values of the ratio of branching ratios  $R_D$  and  $R_{D^*}$  is imposed. The corresponding allowed ranges in  $\mathcal{B}(B_c \rightarrow \tau\nu)$  and  $\mathcal{B}(B_s \rightarrow D_s \tau\nu)$  in the presence of such NP couplings are shown in the right panel. The pink constant line denotes the upper bound of  $\mathcal{B}(B_c \rightarrow \tau\nu) = 30\%$  obtained in the SM.

$\mathcal{B}(B_s \rightarrow D_s \tau \nu)\%$	$R_{D_s}$	$P^\tau$	$A_{FB}^\tau$	$C_F^\tau$
[0.687, 1.176]	[0.305, 0.532]	[-0.201, 0.205]	[0.219, 0.331]	[-0.155, -0.261]

TABLE VII: Allowed ranges of various observables in the presence of  $\tilde{S}_L$  and  $\tilde{S}_R$  NP couplings

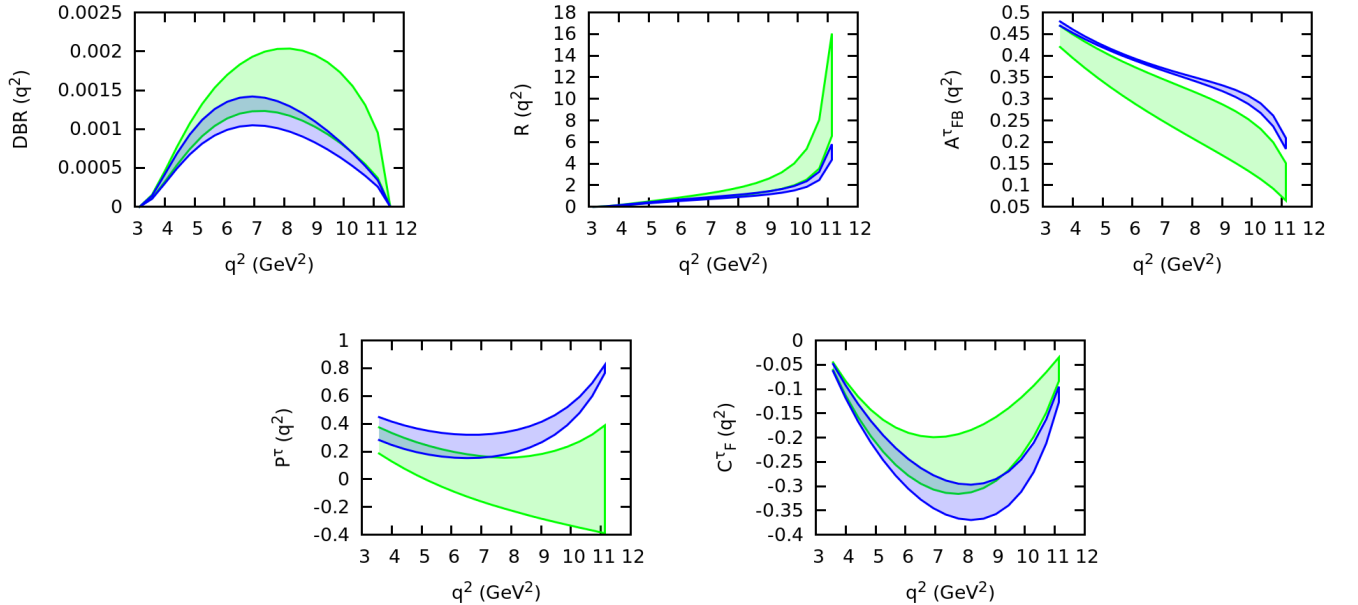


FIG. 9:  $q^2$  dependence of various observables with the allowed ranges of  $\tilde{S}_L$  and  $\tilde{S}_R$  NP couplings of Fig. 8 are shown with green band. The corresponding  $1\sigma$  SM range is shown with the blue band.

## IV. CONCLUSION

In view of the long standing anomalies in  $R_D$  and  $R_{D^*}$ , we study the corresponding  $B_s \rightarrow D_s \tau \nu$  semileptonic decays in a model independent framework. We use the helicity formalism to study the  $B_s \rightarrow D_s \tau \nu$  semileptonic decays within the context of an effective Lagrangian in the presence of NP and explore four different NP scenarios based on contributions coming from two different NP operators. We give prediction on various observables such as branching ratio, ratio of branching ratio, forward backward asymmetry, longitudinal polarization fraction of the charged lepton, and the convexity parameter for this decay mode within SM and within four different NP scenarios.

We first report the central values and the  $1\sigma$  ranges of each observable within the SM for both the  $e$  and the  $\tau$  modes. We notice that all the observables change considerably while going from the  $e$  mode to the  $\tau$  mode. The value of  $R_{D_s}$  is quite similar to the value reported in Ref. [59]. We also give the first prediction of the longitudinal polarization fraction of the charged lepton, lepton side forward backward asymmetry, and the convexity parameter for the  $B_s \rightarrow D_s l \nu$  decays.

For our NP analysis, we assume that NP effects are coming from vector and scalar type NP couplings only. We notice that NP scenarios with  $(V_L, V_R)$  and  $(\tilde{V}_L, \tilde{V}_R)$  NP couplings are compatible with the  $\mathcal{B}(B_c \rightarrow \tau \nu)$  constraint. However, NP scenarios with  $(S_L, S_R)$  and  $(\tilde{S}_L, \tilde{S}_R)$  NP couplings are ruled out due to the constraint coming from the lifetime of  $B_c$  meson.

Study of  $B_s \rightarrow D_s \tau \nu$  decays both theoretically and experimentally is crucial because it may provide new insights into the  $R_D$  and  $R_{D^*}$  anomaly as this decay mode is mediated via the same  $b \rightarrow c$  charged current interaction. Moreover, a precise determination of the branching fractions of this decay mode will allow an accurate determination of the CKM matrix element  $|V_{cb}|$ .

- 
- [1] G. Ciezarek, M. Franco Sevilla, B. Hamilton, R. Kowalewski, T. Kuhr, V. Lth and Y. Sato, “A Challenge to Lepton Universality in B Meson Decays,” *Nature* **546**, 227 (2017) doi:10.1038/nature22346 [arXiv:1703.01766 [hep-ex]].
  - [2] J. A. Bailey *et al.* [MILC Collaboration], “BD form factors at nonzero recoil and  $|V_{cb}|$  from 2+1-flavor lattice QCD,” *Phys. Rev. D* **92**, no. 3, 034506 (2015) doi:10.1103/PhysRevD.92.034506 [arXiv:1503.07237 [hep-lat]].
  - [3] H. Na *et al.* [HPQCD Collaboration], “ $B \rightarrow D l \nu$  form factors at nonzero recoil and extraction of  $|V_{cb}|$ ,” *Phys. Rev. D* **92**, no. 5, 054510 (2015) Erratum: [*Phys. Rev. D* **93**, no. 11, 119906 (2016)] doi:10.1103/PhysRevD.93.119906, 10.1103/PhysRevD.92.054510 [arXiv:1505.03925 [hep-lat]].
  - [4] S. Aoki *et al.*, “Review of lattice results concerning low-energy particle physics,” *Eur. Phys. J. C* **77**, no. 2, 112 (2017) doi:10.1140/epjc/s10052-016-4509-7 [arXiv:1607.00299 [hep-lat]].
  - [5] D. Bigi and P. Gambino, “Revisiting  $B \rightarrow D l \nu$ ,” *Phys. Rev. D* **94**, no. 9, 094008 (2016) doi:10.1103/PhysRevD.94.094008 [arXiv:1606.08030 [hep-ph]].
  - [6] S. Fajfer, J. F. Kamenik and I. Nisandzic, “On the  $B \rightarrow D^* \tau \bar{\nu}_\tau$  Sensitivity to New Physics,” *Phys. Rev. D* **85**, 094025 (2012) doi:10.1103/PhysRevD.85.094025 [arXiv:1203.2654 [hep-ph]].
  - [7] J. P. Lees *et al.* [BaBar Collaboration], “Measurement of an Excess of  $\bar{B} \rightarrow D^{(*)} \tau^- \bar{\nu}_\tau$  Decays and Implications for Charged Higgs Bosons,” *Phys. Rev. D* **88**, no. 7, 072012 (2013) doi:10.1103/PhysRevD.88.072012 [arXiv:1303.0571 [hep-ex]].
  - [8] M. Huschle *et al.* [Belle Collaboration], “Measurement of the branching ratio of  $\bar{B} \rightarrow D^{(*)} \tau^- \bar{\nu}_\tau$  relative to  $\bar{B} \rightarrow D^{(*)} \ell^- \bar{\nu}_\ell$  decays with hadronic tagging at Belle,” *Phys. Rev. D* **92**, no. 7, 072014 (2015) doi:10.1103/PhysRevD.92.072014 [arXiv:1507.03233 [hep-ex]].
  - [9] Y. Sato *et al.* [Belle Collaboration], “Measurement of the branching ratio of  $\bar{B}^0 \rightarrow D^{*+} \tau^- \bar{\nu}_\tau$  relative to  $\bar{B}^0 \rightarrow D^{*+} \ell^- \bar{\nu}_\ell$  decays with a semileptonic tagging method,” *Phys. Rev. D* **94**, no. 7, 072007 (2016) doi:10.1103/PhysRevD.94.072007 [arXiv:1607.07923 [hep-ex]].
  - [10] S. Hirose *et al.* [Belle Collaboration], “Measurement of the  $\tau$  lepton polarization and  $R(D^*)$  in the decay  $\bar{B} \rightarrow D^* \tau^- \bar{\nu}_\tau$ ,” *Phys. Rev. Lett.* **118**, no. 21, 211801 (2017) doi:10.1103/PhysRevLett.118.211801 [arXiv:1612.00529 [hep-ex]].
  - [11] R. Aaij *et al.* [LHCb Collaboration], “Measurement of the ratio of branching fractions  $\mathcal{B}(\bar{B}^0 \rightarrow D^{*+} \tau^- \bar{\nu}_\tau)/\mathcal{B}(\bar{B}^0 \rightarrow D^{*+} \mu^- \bar{\nu}_\mu)$ ,” *Phys. Rev. Lett.* **115**, no. 11, 111803 (2015) Erratum: [*Phys. Rev. Lett.* **115**, no. 15, 159901 (2015)] doi:10.1103/PhysRevLett.115.159901, 10.1103/PhysRevLett.115.111803 [arXiv:1506.08614 [hep-ex]].
  - [12] Y. Amhis *et al.* [HFLAV Collaboration], “Averages of  $b$ -hadron,  $c$ -hadron, and  $\tau$ -lepton properties as of summer 2016,” *Eur. Phys. J. C* **77**, no. 12, 895 (2017) doi:10.1140/epjc/s10052-017-5058-4 [arXiv:1612.07233 [hep-ex]].
  - [13] R. Dutta, A. Bhol and A. K. Giri, “Effective theory approach to new physics in  $b \rightarrow u$  and  $b \rightarrow c$  leptonic and semileptonic decays,” *Phys. Rev. D* **88**, no. 11, 114023 (2013) doi:10.1103/PhysRevD.88.114023 [arXiv:1307.6653 [hep-ph]].
  - [14] A. Celis, M. Jung, X. Q. Li and A. Pich, “Sensitivity to charged scalars in  $B \rightarrow D^{(*)} \tau \nu_\tau$  and  $B \rightarrow \tau \nu_\tau$  decays,” *JHEP* **1301**, 054 (2013) doi:10.1007/JHEP01(2013)054 [arXiv:1210.8443 [hep-ph]].
  - [15] R. Dutta and A. Bhol, “ $b \rightarrow (c, u), \tau \nu$  leptonic and semileptonic decays within an effective field theory approach,” *Phys. Rev. D* **96**, no. 3, 036012 (2017) doi:10.1103/PhysRevD.96.036012 [arXiv:1611.00231 [hep-ph]].

- [16] A. K. Alok, D. Kumar, S. Kumbhakar and S. U. Sankar, “ $D^*$  polarization as a probe to discriminate new physics in  $\bar{B} \rightarrow D^* \tau \bar{\nu}$ ,” Phys. Rev. D **95**, no. 11, 115038 (2017) doi:10.1103/PhysRevD.95.115038 [arXiv:1606.03164 [hep-ph]].
- [17] M. A. Ivanov, J. G. Krner and C. T. Tran, “Analyzing new physics in the decays  $\bar{B}^0 \rightarrow D^{(*)} \tau^- \bar{\nu}_\tau$  with form factors obtained from the covariant quark model,” Phys. Rev. D **94**, no. 9, 094028 (2016) doi:10.1103/PhysRevD.94.094028 [arXiv:1607.02932 [hep-ph]].
- [18] C. T. Tran, M. A. Ivanov and J. G. Krner, “Analyzing New Physics in  $\bar{B}^0 \rightarrow D^{(*)} \tau^- \bar{\nu}_\tau$ ,” arXiv:1702.06910 [hep-ph].
- [19] A. Celis, M. Jung, X. Q. Li and A. Pich, “Scalar contributions to  $b \rightarrow c(u) \tau \nu$  transitions,” Phys. Lett. B **771**, 168 (2017) doi:10.1016/j.physletb.2017.05.037 [arXiv:1612.07757 [hep-ph]].
- [20] L. Dhargyal, “Explaining the observed deviation in  $R(D^{(*)})$  and  $\text{Br}(B \rightarrow \tau \nu_\tau)$  in an anomalous 2HDM,” arXiv:1610.06291 [hep-ph].
- [21] P. Colangelo and F. De Fazio, “Scrutinizing  $\bar{B} \rightarrow D^*(D\pi) \ell^- \bar{\nu}_\ell$  and  $\bar{B} \rightarrow D^*(D\gamma) \ell^- \bar{\nu}_\ell$  in search of new physics footprints,” arXiv:1801.10468 [hep-ph].
- [22] M. Tanaka, “Charged Higgs effects on exclusive semitauonic  $B$  decays,” Z. Phys. C **67**, 321 (1995) doi:10.1007/BF01571294 [hep-ph/9411405].
- [23] U. Nierste, S. Trine and S. Westhoff, “Charged-Higgs effects in a new  $B \rightarrow \tau \nu$  differential decay distribution,” Phys. Rev. D **78**, 015006 (2008) doi:10.1103/PhysRevD.78.015006 [arXiv:0801.4938 [hep-ph]].
- [24] T. Miki, T. Miura and M. Tanaka, “Effects of charged Higgs boson and QCD corrections in anti- $B \rightarrow \tau \nu$ ,” hep-ph/0210051.
- [25] S. Fajfer, J. F. Kamenik, I. Nisandzic and J. Zupan, “Implications of Lepton Flavor Universality Violations in  $B$  Decays,” Phys. Rev. Lett. **109**, 161801 (2012) doi:10.1103/PhysRevLett.109.161801 [arXiv:1206.1872 [hep-ph]].
- [26] A. Crivellin, C. Greub and A. Kokulu, “Explaining  $B \rightarrow D \tau \nu$ ,  $B \rightarrow D^* \tau \nu$  and  $B \rightarrow \tau \nu$  in a 2HDM of type III,” Phys. Rev. D **86**, 054014 (2012) doi:10.1103/PhysRevD.86.054014 [arXiv:1206.2634 [hep-ph]].
- [27] A. Datta, M. Duraisamy and D. Ghosh, “Diagnosing New Physics in  $b \rightarrow c \tau \nu_\tau$  decays in the light of the recent BaBar result,” Phys. Rev. D **86**, 034027 (2012) doi:10.1103/PhysRevD.86.034027 [arXiv:1206.3760 [hep-ph]].
- [28] M. Duraisamy and A. Datta, “The Full  $B \rightarrow D^* \tau^- \bar{\nu}_\tau$  Angular Distribution and CP violating Triple Products,” JHEP **1309**, 059 (2013) doi:10.1007/JHEP09(2013)059 [arXiv:1302.7031 [hep-ph]].
- [29] M. Duraisamy, P. Sharma and A. Datta, “Azimuthal  $B \rightarrow D^* \tau^- \bar{\nu}_\tau$  angular distribution with tensor operators,” Phys. Rev. D **90**, no. 7, 074013 (2014) doi:10.1103/PhysRevD.90.074013 [arXiv:1405.3719 [hep-ph]].
- [30] P. Biancofiore, P. Colangelo and F. De Fazio, “On the anomalous enhancement observed in  $B \rightarrow D^{(*)} \tau \bar{\nu}_\tau$  decays,” Phys. Rev. D **87**, no. 7, 074010 (2013) doi:10.1103/PhysRevD.87.074010 [arXiv:1302.1042 [hep-ph]].
- [31] X. G. He and G. Valencia, “ $B$  decays with  $\tau$  leptons in nonuniversal left-right models,” Phys. Rev. D **87**, no. 1, 014014 (2013) doi:10.1103/PhysRevD.87.014014 [arXiv:1211.0348 [hep-ph]].
- [32] N. G. Deshpande and X. G. He, “Consequences of R-parity violating interactions for anomalies in  $\bar{B} \rightarrow D^{(*)} \tau \bar{\nu}$  and  $b \rightarrow s \mu^+ \mu^-$ ,” Eur. Phys. J. C **77**, no. 2, 134 (2017) doi:10.1140/epjc/s10052-017-4707-y [arXiv:1608.04817 [hep-ph]].
- [33] X. Q. Li, Y. D. Yang and X. Zhang, “Revisiting the one leptoquark solution to the  $R(D^{(0)})$  anomalies and its phenomenological implications,” JHEP **1608**, 054 (2016) doi:10.1007/JHEP08(2016)054 [arXiv:1605.09308 [hep-ph]].
- [34] D. Bardhan, P. Byakti and D. Ghosh, “A closer look at the  $R_D$  and  $R_{D^*}$  anomalies,” JHEP **1701**, 125 (2017) doi:10.1007/JHEP01(2017)125 [arXiv:1610.03038 [hep-ph]].
- [35] M. A. Ivanov, J. G. Krner and C. T. Tran, “Exclusive decays  $B \rightarrow \ell^- \bar{\nu}$  and  $B \rightarrow D^{(*)} \ell^- \bar{\nu}$  in the covariant quark model,” Phys. Rev. D **92**, no. 11, 114022 (2015) doi:10.1103/PhysRevD.92.114022 [arXiv:1508.02678 [hep-ph]].
- [36] S. Nandi, S. K. Patra and A. Soni, “Correlating new physics signals in  $B \rightarrow D^{(*)} \tau \nu_\tau$  with  $B \rightarrow \tau \nu_\tau$ ,” arXiv:1605.07191 [hep-ph].
- [37] R. Alonso, B. Grinstein and J. Martin Camalich, “Lifetime of  $B_c^-$  Constrains Explanations for Anomalies in  $B \rightarrow D^{(*)} \tau \nu$ ,” Phys. Rev. Lett. **118**, no. 8, 081802 (2017) doi:10.1103/PhysRevLett.118.081802 [arXiv:1611.06676 [hep-ph]].
- [38] W. Altmannshofer, P. S. Bhupal Dev and A. Soni, “ $R_{D^{(*)}}$  anomaly: A possible hint for natural supersymmetry with  $R$ -parity violation,” Phys. Rev. D **96**, no. 9, 095010 (2017) doi:10.1103/PhysRevD.96.095010 [arXiv:1704.06659 [hep-ph]].
- [39] S. Iguro and K. Tobe, “ $R(D^{(*)})$  in a general two Higgs doublet model,” Nucl. Phys. B **925**, 560 (2017) doi:10.1016/j.nuclphysb.2017.10.014 [arXiv:1708.06176 [hep-ph]].
- [40] F. U. Bernlochner, Z. Ligeti, M. Papucci and D. J. Robinson, “Combined analysis of semileptonic  $B$  decays to  $D$  and  $D^*$ :  $R(D^{(*)})$ ,  $|V_{cb}|$ , and new physics,” Phys. Rev. D **95**, no. 11, 115008 (2017) doi:10.1103/PhysRevD.95.115008 [arXiv:1703.05330 [hep-ph]].
- [41] S. Bhattacharya, S. Nandi and S. K. Patra, “Looking for possible new physics in  $B \rightarrow D^{(*)} \tau \nu_\tau$  in light of recent data,” Phys. Rev. D **95**, no. 7, 075012 (2017) doi:10.1103/PhysRevD.95.075012 [arXiv:1611.04605 [hep-ph]].
- [42] R. Aaij *et al.* [LHCb Collaboration], “Measurement of the ratio of branching fractions  $\mathcal{B}(B_c^+ \rightarrow J/\psi \tau^+ \nu_\tau)/\mathcal{B}(B_c^+ \rightarrow J/\psi \mu^+ \nu_\mu)$ ,” arXiv:1711.05623 [hep-ex].
- [43] M. A. Ivanov, J. G. Korner and P. Santorelli, “Semileptonic decays of  $B_c$  mesons into charmonium states in a relativistic quark model,” Phys. Rev. D **71**, 094006 (2005) Erratum: [Phys. Rev. D **75**, 019901 (2007)] doi:10.1103/PhysRevD.75.019901, 10.1103/PhysRevD.71.094006 [hep-ph/0501051].
- [44] W. F. Wang, Y. Y. Fan and Z. J. Xiao, “Semileptonic decays  $B_c \rightarrow (\eta_c, J/\Psi) \ell \nu$  in the perturbative QCD approach,” Chin. Phys. C **37**, 093102 (2013) doi:10.1088/1674-1137/37/9/093102 [arXiv:1212.5903 [hep-ph]].
- [45] R. Dutta and A. Bhol, “ $B_c \rightarrow (J/\psi, \eta_c) \tau \nu$  semileptonic decays within the standard model and beyond,” Phys. Rev. D **96**, no. 7, 076001 (2017) doi:10.1103/PhysRevD.96.076001 [arXiv:1701.08598 [hep-ph]].

- [46] A. Lytle, B. Colquhoun, C. Davies, J. Koponen and C. McNeile, PoS BEAUTY **2016**, 069 (2016) [arXiv:1605.05645 [hep-lat]].
- [47] M. Atoui, D. Becirevic, V. Mornas and F. Sanfilippo, “Lattice QCD study of  $B_s \rightarrow D_s \ell \bar{\nu}_\ell$  decay near zero recoil,” PoS LATTICE **2013**, 384 (2014) [arXiv:1311.5071 [hep-lat]].
- [48] M. Atoui, V. Mornas, D. Beirevic and F. Sanfilippo, “ $B_s \rightarrow D_s \ell \nu_\ell$  near zero recoil in and beyond the Standard Model,” Eur. Phys. J. C **74**, no. 5, 2861 (2014) doi:10.1140/epjc/s10052-014-2861-z [arXiv:1310.5238 [hep-lat]].
- [49] J. A. Bailey *et al.*, “ $B_s \rightarrow D_s/B \rightarrow D$  Semileptonic Form-Factor Ratios and Their Application to  $\text{BR}(B_s^0 \rightarrow \mu^+ \mu^-)$ ,” Phys. Rev. D **85**, 114502 (2012) Erratum: [Phys. Rev. D **86**, 039904 (2012)] doi:10.1103/PhysRevD.85.114502, 10.1103/PhysRevD.86.039904 [arXiv:1202.6346 [hep-lat]].
- [50] S. M. Zhao, X. Liu and S. J. Li, “Study on  $B(s) \rightarrow \ell D(sJ) (2317, 2460) 1$  anti- $\nu$  Semileptonic Decays in the CQM Model,” Eur. Phys. J. C **51**, 601 (2007) doi:10.1140/epjc/s10052-007-0322-7 [hep-ph/0612008].
- [51] A. Bhol, “Study of  $B_s \rightarrow D_s^{(*)} \ell \nu_\ell$  semileptonic decays,” EPL **106**, no. 3, 31001 (2014). doi:10.1209/0295-5075/106/31001
- [52] X. J. Chen, H. F. Fu, C. S. Kim and G. L. Wang, “Estimating Form Factors of  $B_s \rightarrow D_s^{(*)}$  and their Applications to Semileptonic and Non-leptonic Decays,” J. Phys. G **39**, 045002 (2012) doi:10.1088/0954-3899/39/4/045002 [arXiv:1106.3003 [hep-ph]].
- [53] G. Li, F. I. Shao and W. Wang, “ $B_s \rightarrow D_s(3040)$  form factors and  $B_s$  decays into  $D_s(3040)$ ,” Phys. Rev. D **82**, 094031 (2010) doi:10.1103/PhysRevD.82.094031 [arXiv:1008.3696 [hep-ph]].
- [54] Y. Y. Fan, W. F. Wang and Z. J. Xiao, “Study of  $\bar{B}_s^0 \rightarrow (D_s^+, D_s^{*+}) \ell^- \bar{\nu}_\ell$  decays in the pQCD factorization approach,” Phys. Rev. D **89**, no. 1, 014030 (2014) doi:10.1103/PhysRevD.89.014030 [arXiv:1311.4965 [hep-ph]].
- [55] A. Bazavov *et al.* [MILC Collaboration], “Nonperturbative QCD Simulations with 2+1 Flavors of Improved Staggered Quarks,” Rev. Mod. Phys. **82**, 1349 (2010) doi:10.1103/RevModPhys.82.1349 [arXiv:0903.3598 [hep-lat]].
- [56] H. Na, C. J. Monahan, C. T. H. Davies, R. Horgan, G. P. Lepage and J. Shigemitsu, “The  $B$  and  $B_s$  Meson Decay Constants from Lattice QCD,” Phys. Rev. D **86**, 034506 (2012) doi:10.1103/PhysRevD.86.034506 [arXiv:1202.4914 [hep-lat]].
- [57] C. J. Monahan, H. Na, C. M. Bouchard, G. P. Lepage and J. Shigemitsu, “ $B_{(s)} \rightarrow D_{(s)}$  semileptonic decays with NRQCD-HISQ valence quarks,” PoS LATTICE **2016**, 298 (2016) [arXiv:1611.09667 [hep-lat]].
- [58] R. H. Li, C. D. Lu and Y. M. Wang, “Exclusive  $B(s)$  decays to the charmed mesons  $D(s) + (1968, 2317)$  in the standard model,” Phys. Rev. D **80**, 014005 (2009) doi:10.1103/PhysRevD.80.014005 [arXiv:0905.3259 [hep-ph]].
- [59] C. J. Monahan, H. Na, C. M. Bouchard, G. P. Lepage and J. Shigemitsu, “ $B_s \rightarrow D_s \ell \nu$  Form Factors and the Fragmentation Fraction Ratio  $f_s/f_d$ ,” Phys. Rev. D **95**, no. 11, 114506 (2017) doi:10.1103/PhysRevD.95.114506 [arXiv:1703.09728 [hep-lat]].
- [60] I. I. Y. Bigi, “Inclusive  $B(c)$  decays as a QCD lab,” Phys. Lett. B **371**, 105 (1996) doi:10.1016/0370-2693(95)01574-4 [hep-ph/9510325].
- [61] M. Beneke and G. Buchalla, “The  $B_c$  Meson Lifetime,” Phys. Rev. D **53**, 4991 (1996) doi:10.1103/PhysRevD.53.4991 [hep-ph/9601249].
- [62] C. H. Chang, S. L. Chen, T. F. Feng and X. Q. Li, “The Lifetime of  $B_c$  meson and some relevant problems,” Phys. Rev. D **64**, 014003 (2001) doi:10.1103/PhysRevD.64.014003 [hep-ph/0007162].
- [63] A. G. Akeroyd and C. H. Chen, “Constraint on the branching ratio of  $B_c \rightarrow \tau \bar{\nu}$  from LEP1 and consequences for  $R(D^{(*)})$  anomaly,” Phys. Rev. D **96**, no. 7, 075011 (2017) doi:10.1103/PhysRevD.96.075011 [arXiv:1708.04072 [hep-ph]].
- [64] V. Cirigliano, J. Jenkins and M. Gonzalez-Alonso, “Semileptonic decays of light quarks beyond the Standard Model,” Nucl. Phys. B **830**, 95 (2010) doi:10.1016/j.nuclphysb.2009.12.020 [arXiv:0908.1754 [hep-ph]].
- [65] T. Bhattacharya, V. Cirigliano, S. D. Cohen, A. Filipuzzi, M. Gonzalez-Alonso, M. L. Graesser, R. Gupta and H. W. Lin, “Probing Novel Scalar and Tensor Interactions from (Ultra)Cold Neutrons to the LHC,” Phys. Rev. D **85**, 054512 (2012) doi:10.1103/PhysRevD.85.054512 [arXiv:1110.6448 [hep-ph]].
- [66] J. G. Korner and G. A. Schuler, “Exclusive Semileptonic Heavy Meson Decays Including Lepton Mass Effects,” Z. Phys. C **46**, 93 (1990). doi:10.1007/BF02440838
- [67] A. Kadeer, J. G. Korner and U. Moosbrugger, “Helicity analysis of semileptonic hyperon decays including lepton mass effects,” Eur. Phys. J. C **59**, 27 (2009) doi:10.1140/epjc/s10052-008-0801-5 [hep-ph/0511019].
- [68] C. Patrignani *et al.* [Particle Data Group], “Review of Particle Physics,” Chin. Phys. C **40**, no. 10, 100001 (2016). doi:10.1088/1674-1137/40/10/100001